

Clues to the Metallicity Distribution in the Galactic Bulge: Abundances in OGLE–2007–BLG–349S¹

Judith G. Cohen², Wenjin Huang², A. Udalski⁴, Andrew Gould³ & Jennifer Johnson³

ABSTRACT

We present an abundance analysis based on high dispersion and high signal-to-noise ratio Keck spectra of a very highly microlensed Galactic bulge dwarf, OGLE–2007–BLG–349S, with $T_{\text{eff}} \sim 5400$ K. The amplification at the time the spectra were taken ranged from 350 to 450. This bulge star is highly enhanced in metallicity with $[\text{Fe}/\text{H}]^1 = +0.51 \pm 0.09$ dex. The abundance ratios for the 28 species of 26 elements for which features could be detected in the spectra are solar. In particular, there is no evidence for enhancement of any of the α -elements including O and Mg. We conclude that the high $[\text{Fe}/\text{H}]$ seen in this star, when combined with the equally high $[\text{Fe}/\text{H}]$ derived in previous detailed abundance analysis of two other Galactic bulge dwarfs, both also microlensed, implies that the median metallicity in the Galactic bulge is very high. We thus infer that many previous estimates of the metallicity distribution in the Galactic bulge have substantially underestimated the mean Fe-metallicity there due to sample bias, and suggest a candidate mechanism for such. If our conjecture proves valid, it may be necessary to update the calibrations for the algorithms used by many groups to interpret spectra and broad band photometry of the integrated light of very metal-rich old stellar populations, including luminous elliptical galaxies.

Subject headings: gravitational lensing – stars: abundances – Galaxy: bulge – Galaxy: galaxies – bulges

¹Based in part on observations obtained at the W.M. Keck Observatory, which is operated jointly by the California Institute of Technology, the University of California, and the National Aeronautics and Space Administration.

²Palomar Observatory, Mail Stop 105-24, California Institute of Technology, Pasadena, Ca., 91125, jlc,wenjin@astro.caltech.edu

³Department of Astronomy, Ohio State University, 140 W. 18th Ave., Columbus, OH 43210; gould,jaj@astronomy.ohio-state.edu

⁴Warsaw University Observatory, A1. Ujazdowskie 4, 00-478 Warszawa, Poland; udalski@astrouw.edu.pl,

¹We adopt the usual spectroscopic notations that $[\text{A}/\text{B}] \equiv \log_{10}(N_{\text{A}}/N_{\text{B}})_{*} - \log_{10}(N_{\text{A}}/N_{\text{B}})_{\odot}$, and that $\log[\epsilon(\text{A})] \equiv \log_{10}(N_{\text{A}}/N_{\text{H}}) + 12.00$, for elements A and B .

1. Introduction

Microensing occurs when a “lens” (star, planet, black hole, etc) becomes closely aligned with a more distant “source” star, whose image it both magnifies and distorts. Normally the observer is most interested to learn about the lens, but microensing data can simultaneously serve as a powerful probe of the source. If the source transits the lens (or the “caustics” generated by the lens, in the case of binary lenses), then it resolves the source, allowing detailed limb-darkening profiles from a photometric times series (Fields et al. 2003) or even spectral resolution of surface features like the chromosphere (Cassan et al. 2004) from judiciously taken spectra.

The lens can also serve simply to amplify the role of the telescope as a “light bucket”. Minniti et al. (1998) provocatively titled their report on observations of a bulge dwarf that was magnified by a factor $A = 2.25$ “Using Keck I as a 15m Diameter Telescope”. Obviously, this trick could in principle be improved to arbitrary “diameters” simply by observing the events at higher magnification. The problem is that it is extremely difficult to recognize high-magnification events in advance, and harder still to activate large-telescope observations in time to take advantage of them. The process has been facilitated by microensing planet hunters, who prize high-magnification events because of their extreme sensitivity to planets (Udalski et al. 2005; Gould et al. 2006). Johnson et al. (2007) were the first to piggy-back on the microensing planet hunters, obtaining a 15 minute Keck spectrum of the Galactic bulge dwarf OGLE–2006–BLG–265S at magnification $A = 135$. This star, the first bulge dwarf with a high-quality spectrum, proved to be extremely metal-rich, a fact that might be telling us that the bulge is much more metal-rich than seems indicated by available spectra of giants, but could also just be the “luck of the draw”. The Johnson et al. (2007) results therefore substantially raised the premium on obtaining highly-magnified spectra of bulge dwarfs.

On 2 July 2007, the OGLE collaboration² (Udalski 2003) announced OGLE–2007–BLG–349 (RA=18:05:24.43; DEC = –26:25:19.0) at Galactic coordinates $(l, b) = (4.4, -2.5)$, i.e., 5.1° from the Galactic center, as a probable microensing event. The Microensing Follow Up Network³ (μ FUN) began monitoring the event on 18 August to determine whether the event would be high-magnification and on 3 September issued a general alert that it would reach at least $A > 200$ two nights hence. On this basis, μ FUN organized world-wide photometric observations, whose outcome will be reported elsewhere (Dong et al. 2008) and also contacted JGC at the Keck telescope to recommend intensive observations.

The ability to obtain high resolution, high quality spectra of Galactic bulge stars and to carry out a detailed abundance analysis offers an unbiased way to determine the metallicity distribution of stars in the Galactic bulge, as well as their detailed chemical inventory. Our abundance analysis of OGLE–2007–BLG–349S is described in the first few sections of the paper, with the key results

²<http://www.astrouw.edu.pl/~ogle/ogle3/ews/ews.html>

³<http://www.astronomy.ohio-state.edu/~microfun/>

presented in §5. In an effort to explain our rather surprising results, we indicate in §6 how past studies of the brightest giants, which are the only bulge stars for which detailed abundance analyses can be derived from spectra obtained under normal conditions, may be subject to previously ignored selection effects. Abundance ratios in the Galactic bulge giants and in the microlensed dwarfs are discussed in §7. Further speculations of the potential impact of our results with regard to the interpretation of the integrated light spectra of metal-rich stellar populations are given in §8. A brief summary concludes the paper, while an appendix discusses the behavior of selected diffuse interstellar bands in the spectrum of OGLE–2007–BLG–349S.

2. Observations

In light of the prediction that the magnification of the presumed Galactic bulge star OGLE–2007–BLG–349S would be very large, we decided to observe the object in an attempt to obtain a high signal-to-noise and high resolution spectrum. The night of 5 September 2007 was clear at the Keck Observatory, and the seeing⁴ was good, 0.8 arcsec in the optical. We found the microlensed star, confirmed that it was bright, and took three consecutive spectra, each 1350 sec in length. The UTCs at the end of each exposure were 06:03:14, 06:27:04 and 06:50:27. HIRES-R (Vogt et al. 1994) was used on the Keck I telescope in a configuration with coverage from 3900 to 8350 Å, with small gaps between the orders beyond 6650 Å. The slit was 0.86 arcsec wide, giving a spectral resolution of 48,000.

The magnifications at the times of the 3 spectra were $A=350$, $A=390$, and $A=450$; apparent I at these times ranged from 13.68 to 13.41 mag (Dong et al. 2008). Hence our observations were carried out at a time when the amplification was larger by a factor of 3 than that of any previous highly magnified star with a high resolution spectrum. While the SNR of the resulting summed spectrum is low for $\lambda < 5000$ Å (~ 30 /spectral resolution element at 4500 Å), not unexpected given the high extinction toward the Galactic bulge, the SNR/spectral resolution element in the continuum at $\lambda > 5500$ Å exceeds 90. Isolated lines with W_λ of 15 mÅ are easily detected at such wavelengths.

According to the microlensing model of Dong et al. (2008), the source passed very close to a cusp shortly (roughly 2 hrs) after the third observation. This means that the limb of the star was magnified more strongly than the center. We have calculated the maximum effect on the $V - I$ color due to differential magnification of the (cooler) limb of the star being more magnified than the center, with limb-darkening included, to be less than 0.005 mag during the spectroscopic exposures, and we ignore it.

⁴The seeing was measured from the profile of the stellar image along the slit in the three individual spectroscopic exposures of OGLE–2007–BLG–349S.

3. Stellar Parameters

We determined T_{eff} for OGLE–2007–BLG–349S in three different ways, from line depth ratios of close pairs of temperature sensitive lines, from Fe I excitation, and from the ionization equilibrium between Fe I and Fe II.

Gray & Johanson (1991) have demonstrated that ratios of the central depth of selected pairs of lines that are close together in wavelength and highly sensitive to temperature can be used to deduce T_{eff} to high accuracy for cool stars. We checked the 15 such line pairs studied by Biazzo, Frasca, Catalano & Marilli (2007). In many cases one or both of the lines were highly saturated in the spectrum of OGLE–2007–BLG–349S, with central depths approaching 70% of the continuum. There were only 3 line pairs for which both lines had central depths of 40% or less. Using their polynomial fit for non-rotating dwarfs, we find a mean T_{eff} from these three pairs of 5350 K.

The Fe abundance was determined from 135 lines of Fe I and 11 of Fe II. As described in detail in §4, $T_{\text{eff}} = 5400$ K produces a deduced Fe abundance independent of the excitation potential of the Fe I line and a difference between $[\text{Fe}/\text{H}]$ from Fe I versus from Fe II lines of only 0.08 dex, well within the expected uncertainty of $|\text{[Fe/H:Fe I]} - \text{[Fe/H:Fe II]}|$.

These three methods give a mean T_{eff} of 5431 K, with $\sigma = 72$ K. We adopt $T_{\text{eff}} = 5400 \pm 100$ K. The extinction corrected $V - I$ color can be determined from the light curve of the microlensed star. The extinction to the source is taken to be that of the red clump stars on the horizontal branch in the neighborhood of the source, which is determined from OGLE II publicly available multi-color photometry. We assume that there is no differential extinction between the adjacent bulge red clump stars⁵ and the target. With this extinction, the model of Dong et al. (2008) that fits the two-color (V and I , where the latter is in the Cousins system) microlensing light curve for OGLE–2007–BLG–349S fixes the flux level of the source to be $I_0 = 18.72$ mag with $(V - I)_0 = 0.73$ mag. Because the lens lies in the foreground disk (Dong et al. 2008), the most probable distance to the source is that of the Galactic center, 8.0 kpc. The absolute magnitude is then $M_I = 4.22$. The bulge star is thus slightly fainter and slightly redder than the Sun ($V - I = 0.688 \pm 0.014$ mag, Holmberg, Flynn & Portinari 2006). Combining this with the colors of stars along a metal-rich isochrone of Yi et al. (2001) suggests $T_{\text{eff}} = 5550$ K, 1.5σ hotter than our adopted T_{eff} . If the extinction corrected $V - I$ color determined in this way is underestimated by 0.08 mag (of which 0.05 mag may arise from an underestimate of the intrinsic color of the red clump) as was suspected by Johnson et al. (2007), who employed exactly the same method for OGLE–2006–BLG–265S, then the deduced T_{eff} for OGLE–2007–BLG–349S would be ~ 5430 K, essentially identical to that deduced from the spectrum itself.

We next turn to the surface gravity. With T_{eff} set, we can determine $\log(g)$ from the ionization

⁵The dereddened red clump in the Galactic bulge is assumed to have $I_0 = 14.32$ mag and $(V - I)_0 = 1.00$ mag.

equilibrium between Fe I and Fe II, from an isochrone, and from the line profile in the damping wings of a very strong line. The Galactic bulge is old (see, for example, Ortolani et al. 1995). We assume the age of OGLE–2007–BLG–349S is 9 Gyr. From the isochrones of Yi et al. (2001), we find that the main sequence turnoff occurs at 5500 K for $Z = 0.04$ (a metallicity 2.4 times solar) and no α -enhancement at an age of 9 Gyr. A star at 5400 K can be a subgiant with $\log(g) = 4.0$ dex, or a dwarf below the turnoff with $\log(g) = 4.4$ dex. For an upper main sequence star with a fixed T_{eff} , $\log(g)$ decreases by ~ 0.15 dex when the isochrone age is changed from 4 to 9 Gyr. Similarly, $\log(g)$ for a fixed age within this interval and metallicity ranging from $z = 0.00$ to $z = 0.06$ increases by ~ 0.10 dex. Thus our choice of an age of 9 Gyr for the isochrone we adopt to determine $\log(g)$ is not crucial, nor is the exact choice of metallicity of the isochrone.

Profiles of very strong lines with obvious damping wings can constrain $\log(g)$. Figure 1 shows a spectral synthesis in the region of the 6162.2 Å line of Ca I. A synthesis of the solar spectrum with the same line list gives a very good fit. The best fit for $\log(g)$ is 4.35 dex, supporting OGLE–2007–BLG–349S being a dwarf rather than a subgiant. Note that a solar [Ca/Fe] ratio and [Fe/H] = +0.5 dex is assumed for this synthesis. In addition, the M_I of 4.22 mag deduced from the extinction combined with the microlensing light curve is 0.1 mag brighter than that of a 5400 K dwarf with this isochrone, but is 1.0 mag fainter than that of a subgiant from that isochrone with that T_{eff} . The predicted number density for dwarfs as compared to subgiants is about 4:1 for a Salpeter IMF, further favoring the star being a dwarf. We thus feel confident that OGLE–2007–BLG–349S is a dwarf just below the main sequence turnoff with $\log(g) \sim 4.4$ dex. The ionization equilibrium between Fe I and Fe II is satisfactory at $\log(g) = 4.5$ dex. The uncertainty in T_{eff} of 100 K translates into an uncertainty in $\log(g)$ of 0.2 dex. We adopt $\log(g) = 4.5 \pm 0.2$ dex for the abundance analysis.

4. Abundance Analysis

Our Keck/HIRES spectrum of OGLE–2007–BLG–349S is full of strong lines with considerable blending and crowding, especially in the blue. Fe I lines at $\lambda < 5900$ Å were ignored, as were Fe II lines blueward of 5100 Å. For all other species, lines blueward of 5200 Å were excluded. A line list for Fe I and Fe II was assembled from that used by Fulbright, McWilliam & Rich (2006) in their study of K giants in Baade’s window and from JGC’s personal line list, augmented by selected very weak isolated lines found in the solar spectrum. Equivalent widths and atomic parameters for the lines used are given in Table 1. Lines with $W_\lambda > 180$ mÅ were rejected unless the species has very few detected features; those retained that are stronger than this are the only detected line of K I and the 5680 Å Na I doublet. (The NaD lines are much too strong to consider using and are hopelessly contaminated with interstellar absorption.) Equivalent widths were measured using an automatic Gaussian fitting routine combined with the measured heliocentric v_r of $+99.47 \pm 0.05$ km s $^{-1}$. The stronger lines were all checked by hand to make sure the damping wings were picked up when appropriate. The Mg I triplet lines in the region of 6320 Å, where there is a broad autoionization

feature of Ca, were measured by hand. For elements with only a few detected lines, all features were checked by hand as well. The FTS solar spectrum of Wallace, Hinkle & Livingston (1998), available online, was very useful for this purpose. The major uncertainty in the W_λ results from the definition of the continuum in the crowded spectrum of OGLE–2007–BLG–349S.

The abundance analysis was carried out differentially with respect to the Sun, since the T_{eff} difference is only ~ 400 K, and both stars are dwarfs. We used a current version of the LTE spectral synthesis program MOOG (Snedden 1973). We employ the grid of stellar atmospheres from Kurucz (1993) with $[\text{Fe}/\text{H}] = +0.5$ dex and solar abundance ratios without convective overshoot (Castelli & Kurucz 2003) and with the most recent opacity distribution functions. For consistency, the solar model was taken from the appropriate grid of Kurucz as well.

Spectral syntheses were used for the S I doublet near 6750 \AA and for the Rb I resonance line near 7800 \AA , which lies in the red wing of a much stronger Si I line. A synthesis of the CH band near 4320 \AA using the molecular line list of Jorgensen et al. (1996) was carried out to determine the C abundances.

Transition probabilities from the NIST Atomic Spectra Database Version 3.1 (Ralchenko et al. 2007) were used in general when available. Since we analyze OGLE–2007–BLG–349S differentially with respect to the Sun, the adopted gf values are not crucial, but when “accurate” values are available, we used them. Accurate gf values could not be located for a small number of lines for which we were forced to resort to an inverted solar analysis to assign such; these cases are indicated in Table 1. We used damping constants from Barklem, Piskunov & O’Mara (2000) when available.

We set the microturbulent velocity v_t to 1.0 km s^{-1} , following the example of the Sun. This gave deduced Fe abundances independent of W_λ to within the accuracy that the resulting set of $\log[\epsilon(\text{Fe})]$ from each of Fe I lines could be measured. Hyperfine structure corrections were used for the lines of Ba II, Co I, Cu I, Mn I, Sc II, and V I. These were taken from the compilation generated by Prochaska et al. (2000).

Non-LTE corrections were not generally included, as this is a differential analysis with respect to Sun, and the stellar parameters of OGLE–2007–BLG–349S are fairly close to those of the Sun. Two key elements for which this might be an issue are the 7770 \AA O I triplet and our use of the resonance doublet of K I. We have checked the case of O using the fitting formula given in equation (2) of Bensby, Feltzing & Lundstrom (2004). When all the differences between the stellar parameters for the OGLE star and the Sun are taken into account, they yield a negligible difference in the non-LTE correction for this O triplet. Two sets of non-LTE calculations are available for the K I resonance doublet, of which we observed the redder line; the bluer line is in the middle of a strong terrestrial absorption band. The results of the two groups, given in Ivanova & Shimaskii (2000) and in Takeda et al. (2001), are consistent and suggest that for solar metallicity the K abundance of the OGLE star with respect to the Sun from a LTE analysis should be increased by about 0.08 dex to take into account the probable difference in the non-LTE correction for this line. This has been implemented here. However this adopted value must be regarded as still uncertain

since the non-LTE corrections for K are metallicity sensitive, and none are available for super-solar metallicity.

5. Results of the Abundance Analysis

The final deduced abundances for OGLE–2007–BLG–349S for 28 species of 26 elements are given in Table 2. Our derived absolute abundances, the abundances relative to the Sun, and the abundance ratios $[X/Fe]$ are given in this table. The abundance ratios use either Fe I or Fe II as the reference depending on the ionization state and mean excitation potential of the measured lines of species under consideration. The 1σ dispersion around the mean for each species is given as σ_{obs} . This is calculated from the set of differences between the deduced solar abundance for the species in question and that found for OGLE–2007–BLG–349S for each observed line of the species. Thus neither random nor systematic errors in the gf values contribute to σ_{obs} .

While the absolute abundance for a given species listed in Table 2 will be affected by any systematic error in the gf values of the lines we use here, relative abundances $[X/Fe]$ will not since we have carried out a differential analysis with respect to the Sun. An uncertainty for $[X/Fe]$ for each species, σ_{pred} , is calculated summing five terms combined in quadrature representing a change in T_{eff} of 100 K, the corresponding uncertainty in $\log(g)$ of 0.2 dex, a change in v_t of 0.2 km s^{-1} , and a potential 0.25 dex mismatch between $[Fe/H]$ of OGLE–2007–BLG–349S versus the value +0.5 dex of the model atmospheres we are using. The fifth term, the contribution for errors in W_λ , is set to 0.05 dex if only one or two lines were measured; for a larger number of detected lines we adopt $\sigma_{obs}/\sqrt{N(\text{lines})}$ for this term. This is added in quadrature to the other four terms.

Uncertainties in the absolute abundances have only been calculated for Fe as inferred from Fe I and from Fe II lines and are given below.

The sensitivity of the deduced abundances to changes in the stellar parameters or in v_t is shown in Table 3 for absolute abundances and in Table 4 relative abundances $[X/Fe]$. As expected, the latter show much weaker dependences on the choice of stellar parameters etc. These entries were used to generate the values of σ_{pred} in the last column of Table 2. Table 3 shows that the Fe I abundance $\log[\epsilon(Fe)]$ is almost independent of the choice of T_{eff} , increasing by only +0.12 dex when T_{eff} is increased by 250 K. The neutral species of elements with resonance or low-excitation lines (K I, V I, Rb I, and Zr I) show the largest increase in deduced abundance when T_{eff} is increased, while those species with only high excitation lines (the near-IR O triplet, C I, and S I) show the opposite dependence on T_{eff} , as expected.

The ionization equilibrium for Fe for the adopted T_{eff} and $\log(g)$ is good, as is the Fe I excitation equilibrium.

In addition to presenting what we believe to be the first abundance determinations for Rb and for Zr for any star in the Galactic bulge, there are three key results of the detailed abundance

analysis we have carried out of OGLE–2007–BLG–349S. The first is the very high metallicity we derive. We find $[\text{Fe}/\text{H}]$ is $+0.51 \pm 0.09$ dex from 135 Fe I lines and $+0.43 \pm 0.17$ dex from 11 Fe II lines. To achieve a reduction of $[\text{Fe}/\text{H}]$ to $< +0.3$ dex, T_{eff} must be reduced to ~ 5000 K, with a change of $\log(g)$ of $+0.2$ dex for the dwarf or -0.1 dex for the subgiant, for the star to lie on the appropriate isochrone. The Fe ionization equilibrium will then be altered by 0.3 dex for the dwarf case and by somewhat less for the subgiant. This will produce a Fe ionization equilibrium that is so far from equality that the altered set of stellar parameters must be rejected. To achieve solar metallicity and reasonable Fe ionization equilibrium is simply not possible with any set of stellar parameters that lie on the relevant isochrone.

Second the α -elements O and Mg do not show any excess with respect to Fe; oxygen, which is the most abundant α -element, has sub-solar $[\text{O}/\text{Fe}]$. Finally, in all species for which the abundance is regarded as well determined (the notes in the last column of Table 2 indicate the major concerns), there are no credible deviations from the solar ratios.

We note that $[\text{Fe}/\text{H}]$ cannot be affected by mixing of nuclear processed material from the interior of a dwarf or a red giant as none would have been produced up to that stage of stellar evolution. Furthermore, any diffusion of Fe into the more quiescent dwarf as compared to the stirred up outer layers of the giant would be small in such high metallicity stars and would only make the present conundrum of the unexpectedly high $[\text{Fe}/\text{H}]$ we find in OGLE–2007–BLG–349S worse. We also note that the three line ratios we used as one method for determining T_{eff} detailed in §3 each consisted of a V I line paired with either a Fe I, Ni I or Si I line. We find $[\text{V}/\text{Fe}]$ for OGLE–2007–BLG–349S to be $+0.17 \pm 0.14$ dex (Table 2). If this ratio is actually slightly above solar, a slight underestimate of T_{eff} would result from the line ratio method. Underestimating T_{eff} is equivalent to underestimating $[\text{Fe}/\text{H}]$, which again makes the discrepancy with the bulge giants worse.

6. OGLE–2007–BLG–349S and The Metallicity Distribution of the Galactic Bulge

An early attempt to determine the metallicity distribution in the Galactic bulge was that of Sadler, Rich & Terndrup (1996), who used low resolution spectroscopy for 268 bulge giants and red clump stars to derive a mean $[\text{Fe}/\text{H}]$ of -0.11 ± 0.04 dex. Ramírez et al. (2000) studied a sample of M giants in the near-IR; they found a very similar mean $[\text{Fe}/\text{H}]$ of -0.21 dex with a dispersion of 0.30 dex. Zoccali et al. (2003) used extensive optical and near-IR photometry with CMD fitting; they derived a somewhat lower mean $[\text{Fe}/\text{H}]$. In all these cases, the calibration of the metallicity scale relied on Galactic globular clusters. Zoccali et al. (2003) suggest that the differences between several of these studies depend crucially on the abundances adopted for the two highest metallicity GCs with high resolution abundance analyses, NGC 6553 and NGC 6558. $[\text{Fe}/\text{H}]$ values for these two GCs have ranged over more than 0.5 dex in the literature, but since the work of Cohen et al. (1999) and Carretta et al. (2001), who suggested values higher than most previous studies, more recent analyses have settled toward the higher values, see, e.g., Zoccali et al.

(2004) and Alves-Brito et al. (2006).

An early high dispersion spectroscopic study of Galactic bulge K giants is that of McWilliam & Rich (1994), who found a mean $[\text{Fe}/\text{H}]$ in their sample of -0.25 dex. Fulbright, McWilliam & Rich (2006) updates and expands upon this earlier work. They then use their detailed abundance analyses of 27 K giants in Baade’s window to recalibrate the metallicities for the much larger samples of Sadler, Rich & Terndrup (1996) and of Rich (1988). The mean $[\text{Fe}/\text{H}]$ they thus deduce is -0.10 ± 0.04 dex. The median $[\text{Fe}/\text{H}]$ of their sample is also sub-solar. As infrared echelle spectrographs have become available on 8-m class telescopes, high dispersion studies of Galactic bulge giants in the near-IR have become possible, see, e.g., Rich & Origlia (2005), Cunha & Smith (2006) and Rich, Origlia & Valenti (2007). The mean $[\text{Fe}/\text{H}]$ from the sample of M giants studied by Rich, Origlia & Valenti (2007) in the Galactic bulge is well below solar, with $[\text{Fe}/\text{H}] -0.22 \pm 0.01$ dex. The median Fe-metallicity of the small sample of giants with near-IR spectra analyzed by Cunha & Smith (2006) is also slightly below solar metallicity. Since this sample largely overlaps that of Fulbright, McWilliam & Rich (2006) it is not included in the figures.

Very recently, Zoccali et al. (2008) have presented initial results of a survey of Fe-metallicity in the Galactic bulge from spectra with $\lambda/\Delta\lambda = 20,000$ of about 800 stars. They find a radial gradient in $[\text{Fe}/\text{H}]$ within the bulge with the mean value going from $+0.03$ dex at $b = -4^\circ$ to -0.12 dex at $b = -6^\circ$, and a sharp cutoff towards higher metallicities.

All of these samples of Galactic bulge stars are of luminous giants and/or of red clump stars. They all have mean and median $[\text{Fe}/\text{H}]$ values that are slightly sub-solar and are similar to the mean $[\text{Fe}/\text{H}]$ of -0.1 dex found for local disk stars by Allende Prieto et al. (2004). Yet OGLE–2007–BLG–349S, analyzed here, and OGLE–2006–BLG–265S (Johnson et al. 2007), another Galactic bulge microlensed dwarfs with a high quality detailed abundance analysis, both have $[\text{Fe}/\text{H}] \sim +0.5$ dex; the third such star found to date, MOA–2006–BLG–099S with a lower signal-to-noise ratio spectrum, analyzed by Johnson et al. (2008), has a somewhat lower Fe-metallicity, $[\text{Fe}/\text{H}] = +0.36 \pm 0.18$ dex. The comparison between the $[\text{Fe}/\text{H}]$ distribution for the recalibrated sample of Sadler, Rich & Terndrup (1996) by Fulbright, McWilliam & Rich (2006) and the $[\text{Fe}/\text{H}]$ values deduced for these three Galactic bulge dwarfs is shown in Figure 2. While three stars is an uncomfortably small sample, it is difficult to believe that this is consistent with the published metallicity distributions for the Galactic bulge giants and/or red clump stars. The probability that the sample of three stars would have such high $[\text{Fe}/\text{H}]$ values by chance is less than 1% given the $[\text{Fe}/\text{H}]$ distributions of the larger of the relevant studies in the Galactic bulge claiming to have unbiased samples, including Ramírez et al. (2000) with 110 M giants, which must be considered unbiased at the high metallicity end, Sadler, Rich & Terndrup (1996) (268 bulge stars), and the recalibrated version of the latter by Fulbright, McWilliam & Rich (2006). A KS test shows that the probability of finding the three carefully studied microlensed bulge dwarfs at their very high $[\text{Fe}/\text{H}]$ values if the underlying metallicity distribution is that found by Zoccali et al. (2008) from high dispersion spectra of a very large sample of giants in three bulge fields is less than 10^{-4} . This calculation takes into account the radial gradient in the metallicity distribution function found by Zoccali et al.

(2008).

We suggest that sample bias is responsible for this difference. A possible mechanism is the very high mass loss rates predicted to occur at the very high metallicities and moderately high luminosities being discussed here. These are high enough that in an old stellar population, stars are predicted to lose enough mass to peel off the red giant branch (RGB) before reaching the He-flash, which they never go through. Red clump stars, which are burning He in their cores on the horizontal branch, are even more evolved than giants at the RGB tip, and so their evolutionary tracks, once mass loss is properly taken into account may indicate that their expected numbers in an old very-metal rich population may be even more depleted than are luminous first ascent RGB stars. This effect has actually been detected through CMD studies of the extremely metal-rich open cluster NGC 6791 with $[\text{Fe}/\text{H}] +0.45$ dex (Carretta, Bragaglia & Gratton 2007). In this cluster, Kalirai et al. (2007) found a strong relative absence of luminous RGB stars. We propose that this relative paucity of giants on the upper RGB for very metal-rich old populations produces a bias against the highest metallicity stars by preferentially eliminating them from the samples being studied by all previous investigations in the Galactic bulge, which samples consist of one or more of the luminous K giants, luminous M giants, and red clump stars found there.

If this is correct, then the mean bulge metallicity may be comparable to that expected from the radial gradients prevailing within the Galactic disk at a time ~ 5 Gyr ago extrapolated to the Galactic center. It thus may be that at the present time there is a gradient within the solar circle of stellar metallicity with Galactic radius that is roughly comparable to that measured for the interstellar medium (ISM) at present from HII regions by Esteban et al. (2005) and from planetary nebulae (PN) by Maciel, Queiza & Costa (2007). The latter present an estimate of the change of the radial abundance gradient in the Galaxy as a function of time from PN of varying ages. They suggest that the radial abundance gradient in ISM in the Galactic disk was twice as large ~ 5 Gyr ago when the Sun was formed than it is now.

7. Abundance Ratios

Many previous analyses of Galactic bulge K and M giants have found enhanced α/Fe ratios when compared to both the thick and thin disk stars for which very accurate abundance ratios for many elements for large samples exist, see, e.g., Reddy et al. (2003) or Bensby et al. (2005). Abundance ratios help illuminate the star formation history of the bulge, and the contributions to its chemical inventory as a function of time of SNIa, SNII, and AGB stars. The α -enhancement found in Galactic bulge giants has been viewed as an indication that chemical evolution proceeded more rapidly in the Galactic bulge than in either the Galactic thick or thin disk population. In particular, Matteucci & Brocato (1990) discuss the role of O and Mg as probes of the contribution of massive stars; see Ballero et al. (2007) for a current model. McWilliam et al. (2008) revisit this issue, suggesting that metallicity dependent mass loss rates or nucleosynthesis yields may be important in this context. Such findings help to determine the mode of formation of the Galactic

bulge, whether it is a classical bulge or one formed over a longer timescale through secular evolution of the disk. Detailed discussion of these options and references to the relevant theoretical studies can be found in e.g., *Lecureur et al. (2007)*.

Rapidly increasing samples of luminous stars in the bulge, both in terms of numbers of stars analyzed and in terms of the accuracy of the results, are now becoming available. *Fulbright, McWilliam & Rich (2007)* gives a detailed discussion of α -enhancement in their sample of Galactic bulge K giants. They find enhanced $[\text{O}/\text{Fe}]$, $[\text{Mg}/\text{Fe}]$ and $[\text{Al}/\text{Fe}]$ compared both to the solar ratios and to those in both thick and thin disk stars even in super-solar bulge K giants and discuss the different behavior of the hydrostatic (including O and Mg) and explosive (including Si, Ca and Ti) α elements; only the former appear enhanced in the bulge giants. Recently initial results from a major high dispersion spectroscopic survey of Galactic bulge giants and red clump stars being carried out at the VLT have been reported by *Zoccali et al. (2006)* with more details in *Lecureur et al. (2007)*. They present the analysis of a sample of 53 stars selected to span the color range of bulge giants.

However, our analysis of OGLE-2007-BLG-349S (see Table 2) finds $[\text{O}/\text{Fe}]$ and $[\text{Mg}/\text{Fe}]$ have the solar ratio. *Johnson et al. (2007)* find similar low ratios in OGLE-2006-BLG-265S. The third microlensed star, MOA-2006-BLG-099S, shows a small α -enhancement, but the uncertainties are large, and a 1σ deviation toward smaller values would make them consistent with the solar values. Subsolar $[\text{O}/\text{Fe}]$ is found in all three microlensed dwarfs. Figure 3 shows the abundance ratios $[\text{X}/\text{Fe}]$ for each species detected in one of both of the two bulge dwarfs with $[\text{Fe}/\text{H}] \sim +0.5$ dex. Figures 4 and 5 display the abundance ratios for the three microlensed Galactic bulge dwarfs for several elements as a function of $[\text{Fe}/\text{H}]$ as compared to recent results from samples of luminous Galactic bulge giants.

A comparison of $[\text{Mg}/\text{Fe}]$ with $[\text{Al}/\text{Fe}]$ for the two microlensed bulge dwarfs compared to the results from the samples of bulge giants of *Lecureur et al. (2007)* and of *Fulbright, McWilliam & Rich (2007)* is shown in Figure 6. The three microlensed bulge dwarfs lie at the low end of the distribution in $[\text{Mg}/\text{Fe}]$ and at the extreme low end of that for $[\text{Al}/\text{Fe}]$. Also intriguing is that *Lecureur et al. (2007)* finds evidence for variations among the giants of highest metallicity in their sample of $[\text{O}/\text{Fe}]$, $[\text{Na}/\text{Fe}]$, $[\text{Mg}/\text{Fe}]$ and $[\text{Al}/\text{Fe}]$ that substantially exceed their claimed uncertainties. This is accompanied by an anti-correlation between $[\text{O}/\text{Fe}]$ and $[\text{Na}/\text{Fe}]$ and by a correlation of $[\text{Na}/\text{Fe}]$ with $[\text{Al}/\text{Fe}]$, very reminiscent of the star-to-star abundance variations found within Galactic globular clusters.

As is shown in Figs. 4 and 5, the microlensed dwarfs show no sign of α -enhancement, while the bulge giants have $[\text{Mg}/\text{Fe}]$ (as well as $[\text{Na}/\text{Fe}]$ and $[\text{Al}/\text{Fe}]$) enhanced even at super-solar metallicities. What is causing this difference ? Why do the giants show a such large range in $[\text{X}/\text{Fe}]$ for several key light elements ? Are the giants mixed ? Are there substantial non-LTE corrections which are not being included correctly ? Are the T_{eff} values assigned to the giants incorrect ? Are there errors that are larger than expected in the abundance analyses of the giants ?

The key question is which of the two, bulge giants or microlensed bulge dwarfs, best represents

in its atmosphere today the initial chemical inventory of the star, i.e., of the interstellar medium at the time that the star was formed. It must be noted that the study of microlensed Galactic dwarfs can be carried out differentially with respect to the Sun, as we did here, while those of cool giants are forced to rely on Arcturus and/or μ Leo as the reference. Extrapolating non-LTE corrections from a dwarf near the main sequence turnoff in the bulge to the Sun is a small step, but it is a big leap of faith when one must extrapolate from a much cooler reference giant to the Sun. This is a potentially substantial systematic error in the analysis of bulge giants, which may depend on T_{eff} of the star. A probable example of such a systematic error can be seen in the $[\text{Si}/\text{Fe}]$ panel of Figure 3 of Preston et al. (2006), where this abundance ratio, inferred in every star from the same line of Si I, at 3905 Å, changes systematically from about +0.7 to 0.0 dex as T_{eff} increases from 5000 to 6500 K for a sample of very metal-poor RHB stars and red giants. Presumably $[\text{Si}/\text{Fe}]$ is approximately the same for all the stars included in this figure, but some unrecognized systematic error has crept into the analyses so as to produce the strong trend they found for $[\text{Si}/\text{Fe}]$ with T_{eff} .

Dredge up and mixing in the giants is a possible culprit, particularly since Lecureur et al. (2007) found a large range in $[\text{O}/\text{Fe}]$, $[\text{Na}/\text{Fe}]$, $[\text{Mg}/\text{Fe}]$ and $[\text{Al}/\text{Fe}]$ among the most Fe-rich stars in their large sample of bulge giants. However, at least in the globular cluster case at low $[\text{Fe}/\text{H}]$, one sees C burning into N, and sometimes O burning into N as well (Cohen, Briley & Stetson 2002), occasionally with depleted Mg and enhanced Al. The signature of proton burning via the CN cycle, clearly seen in the globular cluster giants, is not apparent in the bulge giants. For this (and other) reasons, Lecureur et al. (2007) rejected mixing as the explanation for the large range they saw in in some abundance ratios.

If larger samples of microlensed Galactic bulge dwarfs continue to show solar ratios of $[\text{Mg}/\text{Fe}]$ and $[\text{Al}/\text{Fe}]$ while samples of bulge giants show in the mean much higher values for each of these elements coupled with a large range for each, even at super-solar metallicity, we would suggest that the true abundance ratios for the light elements, including the α -elements, at high $[\text{Fe}/\text{H}]$ in the Galactic bulge are those of the dwarfs, not the giants.

There are a rapidly increasing number of papers in the literature that explore the chemical evolution of the Galactic bulge using the rich new datasets based on analyses of bulge giants of Fulbright, McWilliam & Rich (2007) and Lecureur et al. (2007). See, as an example of such, Tsujimoto (2007), who discusses the history of infall and outflows in the bulge as compared to the disk and the consequences for chemical evolution of the presence of an AGN at the center of the Galaxy. With only three bulge dwarfs having detailed abundance analyses and accurate abundance ratios at the present time, we defer further discussion of these issues until a larger sample is in hand. We suggest that until this happens, discussion of details of chemical evolution models for the Galactic bulge, which are dependent on, and try to explain the detailed abundance ratios seen in Galactic bulge stars should be undertaken with some degree of caution and sensitivity to the issues raised above.

8. Further Speculations

We infer in §5 and in §6 from the $[\text{Fe}/\text{H}]$ values obtained through detailed abundance analyses of three microlensed bulge dwarfs, OGLE–2007–BLG–349S analyzed here, OGLE–2006–BLG–265S (Johnson et al. 2007) and MOA–2006–BLG–099S (Johnson et al. 2008), that the median $[\text{Fe}/\text{H}]$ in the Galactic bulge is considerably higher than was previously accepted. Furthermore, there is little or no α -enhancement in the abundance ratios of very metal-rich bulge dwarfs, which dominate the stellar population of the Galactic bulge. There are important consequences for the chemical evolution of the Galactic bulge and for extragalactic objects as well if our results set forth at the end of §5 and our conjectures based on these results, described in §6, are correct. The interpretation of spectra and broad band photometry of the integrated light of simple old metal-rich stellar populations such as are believed to exist in luminous elliptical galaxies will be affected. We expect an underestimate of the true Fe-metallicity of such systems to occur with commonly used tools such as Lick indices, calculated with stellar evolutionary tracks and isochrones that ignore mass loss, as is normally the case. We expect an overestimate of the mass-to-light ratio to occur as well if the luminous RGB stars we expect to be present near the RGB tip in a metal-rich population are not present in their expected numbers. as they contribute only a small fraction of the mass, but a larger fraction of the total luminosity.

We have carried out some simple tests to indicate what the maximum effect might be of our proposed scenario. We removed all stars with $L > 1000 L_{\odot}$ from the 9 Gyr $Z = 0.04$ isochrone with no α -enhancement from Yi et al. (2001). We assume a Salpeter IMF and integrate this truncated isochrone for various parameters. We see the changes we have suggested to occur in M/L , $V - K$, and inferred metallicity for old very metal-rich simple stellar populations. We also integrated several of the Lick indices (Mgb, Fe5015, Fe5270, and $\text{H}\beta$) over the original and modified isochrones using the fitting functions of Worthey et al. (1994). Such tests of the behavior of absorption features in the integrated light show only modest changes in the predicted Lick indices, with $\text{H}\beta/\Delta(\text{H}\beta) \sim -[\text{Fe}5015/\Delta(\text{Fe}5015)]/2$. A genuinely high Mg/Fe ratio in the stars themselves, or at least in their atmospheres, seems required. The contribution of the luminous cool RGB tip stars to the blue integrated light is too small to substantially alter the strength of blue stellar absorption features if these stars are absent from the population. However this depends critically on the assumed metallicity sensitivity of the Mg and Fe Lick indices for very cool giants of very high metallicity, which must be regarded as quite uncertain, and well beyond the metallicity range of any Galactic globular cluster calibrator. We anticipate larger changes to occur in the predicted strength of stellar absorption features in the IR, where such stars dominate the integrated light assuming they are present.

Luminous elliptical galaxies are often treated as old simple stellar populations and are believed to have super-solar Fe-metallicities as well as α -enhancements in many cases. Examples abound in the literature, see, e.g., Trager et al. (2000) and Zeigler et al. (2005). The issues concerning the metallicity and α -enhancement in the Galactic bulge discussed above will potentially impact the interpretation of spectra and broad-band photometry of the integrated light of such galax-

ies. We prefer to defer a more detailed discussion until a larger sample of high quality spectra of microlensed bulge dwarfs is in hand to verify our preliminary (and perhaps provocative and premature) conclusions presented in this paper.

9. Summary

We have analyzed a high dispersion spectrum of a microlensed dwarf, OGLE–2007–BLG–349S, in the Galactic bulge. The magnification of this event was very high, HIRES on the 10-m Keck I Telescope was used, the weather was clear with good seeing, and the exposure time was long compared to any previous such data, so the resulting spectrum has a relatively high signal-to-noise ratio.

We stress that in principle the abundance analysis of a upper main sequence dwarf is much easier and less prone to error for spectra of a fixed signal-to-noise ratio than that of a much cooler but much brighter bulge giant with a very complex spectrum full of blends and of strong molecular bands. The advantages of analyzing microlensed bulge stars, for which the required high signal-to-noise ratio can sometimes be achieved, to improving our understanding of the $[\text{Fe}/\text{H}]$ distribution and chemical evolution of the Galactic bulge are large.

We have derived for OGLE–2007–BLG–349S, which we believe to be a dwarf below the main sequence turnoff with $T_{\text{eff}} \sim 5400$ K, a very high Fe-metallicity, $[\text{Fe}/\text{H}] = +0.51 \pm 0.09$ dex. This is very peculiar given that many previous surveys of the metallicity distribution carried out with large samples of K or M giants in the Galactic bulge find both the mean and median $[\text{Fe}/\text{H}]$ to be sub-solar. The two other microlensed Galactic bulge dwarfs studied in detail, OGLE–2006–BLG–265S by Johnson et al. (2007) and MOA–2006–BLG–099S by Johnson et al. (2008), also have very high Fe-metallicities.

In order to produce consistency, we suggest that there is a sampling bias in the bulge giant samples such that very metal-rich giants are strongly depleted. We suggest a physical mechanism for this, the very high mass loss rates expected for such metal-rich old giants can exhaust their envelopes prior to the normal He-flash.

We also find that OGLE–2007–BLG–349S does not show enhancements of the α elements; neither does OGLE–2006–BLG–265S, analyzed by Johnson et al. (2007). However, most bulge giants from samples with high dispersion spectroscopy, e.g. the work of Fulbright, McWilliam & Rich (2007) and particularly those from Lecureur et al. (2007), do show large (and varying from star to star) enhancements of $[\text{Na}/\text{Fe}]$, $[\text{Mg}/\text{Fe}]$ and $[\text{Al}/\text{Fe}]$ even at super-solar metallicities. We suggest that it is the abundances deduced for the microlensed dwarfs that best represent the initial chemical inventory of the interstellar medium at the time these stars formed, while those derived for the bulge giants may not.

We recognize that three stars is a very small sample, but the implications of our results and

inferences for the chemical evolution of the Galactic bulge and for the interpretation of integrated light spectra and broad-band photometry of old simple stellar populations such as luminous elliptical galaxies, are so important that we offer these hypotheses at this time.

The study of additional highly microlensed Galactic bulge dwarfs to increase the sample from just three such stars is clearly urgent. Now that ongoing microlensing surveys make such observations of Galactic bulge dwarfs feasible, we expect substantial improvements in the sample size of high quality spectra for Galactic bulge dwarfs. Suitable high magnification events are rare and lining up the necessary instruments/telescopes/clear weather at just the right time is difficult. Several years may be required to accumulate a suitable sample of spectra of highly microlensed dwarf stars in the Galactic bulge. We are now appropriately positioned to carry out such a time critical program at the Keck Observatory over the next few years, and eagerly look forward to confirmation of our perhaps premature and provocative hypotheses in the not too distant future.

We are grateful to the many people who have worked to make the Keck Telescope and HIRES a reality and to operate and maintain the Keck Observatory. The authors wish to extend special thanks to those of Hawaiian ancestry on whose sacred mountain we are privileged to be guests. Without their generous hospitality, none of the observations presented herein would have been possible.

J.G.C. and W.H. are grateful to NSF grant AST-0507219 to JGC for partial support. Work by A.G. was supported by NSF grant AST-042758. The OGLE project is partially supported by the Polish MNiSW grant N20303032/4275. We thank Manuela Zoccali for providing results in advance of publication on the metallicity distribution function of bulge giants.

10. Appendix A – Diffuse Interstellar Bands

The origin of the diffuse interstellar bands (DIBs) has been a puzzle for more than 30 years; see, e.g., the review by Herbig (1995). Most stars previously studied with high reddening are hot luminous young stars within a cluster embedded in a single cloud complex whose column density varies somewhat over the angular extent of the cloud, such as the IV Cyg association. But the reddening seen for OGLE–2007–BLG–349S ($E(B - V) = 0.68 \pm 0.10$ mag), while not particularly large, results from the many clouds along the line of sight to the Galactic center, and hence is much more representative of the typical ISM. Very little, if any, of this reddening is believed to arise within the Galactic bulge itself.

Because OGLE–2007–BLG–349S is a metal-rich cool dwarf, rather than an O or B star which would normally be used for such work, measurements of the DIBs are difficult and the results more uncertain than would arise for a much less complex hot star spectrum. The very strong and blended stellar absorption features in the blue part of the spectrum made a clear detection of the classical DIB at 4430 Å impossible. Parameters for those interstellar bands that could be detected with

certainty are given in Table 5. They are comparable in strength with those observed for the well studied B7 supergiant HD 183143 whose values are given in Table A1 of Herbig (1995) even though the reddening of this bright star is $E(B - V) = 1.28$ mag, about twice as large as that of OGLE–2007–BLG–349S. Snow & Cohen (1976) have shown that the band strength per grain in the line of sight apparently decreases with increasing grain size, such that dense interstellar clouds are less efficient in producing absorption by DIBs for the same total reddening than are less dense, but more numerous clouds in the line of sight. The very strong DIBs and immense interstellar absorption in the NaD lines in our spectrum of OGLE–2007–BLG–349S should further elucidate this “skin” effect.

REFERENCES

- Allende Prieto, C., Barklem, P. S., Lambert, D. L. & Cunha, K., 2004, A&A, 420, 183
- Alves-Brito, A. et al., 2006, A&A, 460, 269
- Ballero, S. K., Matteucci, F., Origlia, L. & Rich, R. M., 2007, A&A, 467, 123
- Barklem, P. S., Piskunov, N. & O’Mara, B. J., 2000, A&AS, 142, 467
- Bensby, T., Feltzing, S. & Lundstrom, I., 2004, A&A, 415, 155
- Bensby, T., Feltzing, S., Lundstrom, I. & Ilyin, I., 2005, A&A, 433, 185
- Biazzo, K., Frasca, A., Catalano S. & Marilli E., 2007, Astr. Nach., 328, 938
- Carretta, E., Cohen, J. G., Gratton, R. G. & Behr, B., 2001, AJ, 122, 1469
- Carretta, E., Bragaglia, A. & Gratton, R. G., 2007, A&A, 473, 129
- Cassan, A. et al. 2004, A&A, 419, L1
- Castelli, F. & Kurucz, R. L., 2003, in Poster Paper A20, on CD from IAU Sym. 210, *Modeling of Stellar Atmospheres*, ed. N. E. Piskunov, W. W. Weiss & D. G. Gray (San Francisco: ASP) (see astro-ph/0405087)
- Cohen, J. G., Gratton, R. G., Behr, B. & Carretta, E., 1999, ApJ, 523, 739
- Cohen, J. G., Briley, M. M. & Stetson, P. B., 2002, AJ, 123, 2525
- Cohen, J. G., Christlieb, N., McWilliam, A., Shectman, S., Thompson, I., Wasserburg, G. J., Ivans, I., Dehn, Karlsson, T. & Melendez, J., 2004, ApJ, 612, 1107
- Cunha, K. & Smith, V. V., 2006, ApJ, 651, 49
- Dong, S. et al., 2008, in preparation
- Esteban, C., Garcia-Rojas, J., Peimbert, M., Peimbert, A., Ruiz, M. T., Rodriguez, M. & Carigo, L., 2005, ApJ, 618, L95
- Fields, D.L. et al. 2003, ApJ, 596, 1305
- Fulbright, J. P., McWilliam, A. & Rich, R. M., 2006, ApJ, 636, 821
- Fulbright, J. P., McWilliam, A. & Rich, R. M., 2007, ApJ, in press
- Gould, A., et al. 2006, ApJ, 644, L37
- Gratton, R. G., Sneden, C. & Carretta, E., 2004, ARA&A, 42, 385

- Gray, D.F. & Johanson, H. L., 1991, *ApJ*, 103, 439
- Herbig, G. H., 1995, *ARA&A*, 33, 19
- Holmberg, J., Flynn, C. & Portinari, L., 2006, *MNRAS*, 367, 449
- Houdashelt, M. L., Bell, R. A. & Sweigart, A. V., 2000, *AJ*, 119, 1448
- Ivanova, D. V. & Shimanskii, V. V., 2000, *Astronomy Reports*, 44, 376
- Johnson, J. A., Gal-Yam, A., Leonard, D. C., Simon, J. D., Udalski, A. & Gould, A., 2007, *ApJ*, 655, L3
- Johnson, J. A., Gaido, B.S., Sumi, T., Bond, I. A. & Gould, A., 2008, *ApJ*, submitted
- Jorgensen, U. G., Larsson, M., Iwamae, A. & Yu, B., 1996, *A&A*, 315, 204
- Kalirai, J. S., Bergeron, P., Hansen, B. M. S., Kelson, D. D., Reitzel, D. B., Rich, R. M. & Richer, H. B., 2007, *ApJ*
- Kurucz, R. L., 1993, *ATLAS9 Stellar Atmosphere Programs and 2 km/s Grid*, (Kurucz CD-ROM No. 13)
- Lecureur, A., Hill, V., Zoccali, M., Barbuy, B., Gomez, A., Minniti, D., Ortolani, S. & Renzini, A., 2007, *A&A*, 465, 799
- Maciel, W. J., Quireza, C. & Costa, R. D. D., 2007, *A&A Letters*, in press
- Matteucci, F. & Brocato, E., 1990, *ApJ*, 365, 539
- McWilliam, A. & Rich, R.M., 1994, *ApJS*, 91, 749
- McWilliam, A., Matteucci, F., Ballero, S., Rich, R. M., Fulbright, J. P. & Cescutti, G., 2008, *AJ* (submitted) (Astro-ph/0708.4026)
- Minniti, D., Vandehei, T., Cook, K.H., Griest, K., & Alcock, C. 1998, *ApJ*, 499, L175
- Ortolani, S., Renzini, A., Gilmozzi, R., Marconi, G., Barbuy, B., Bica, E. & Rich, R. M., 1995, *Nature*, 377, 701
- Preston, G. W., Sneden, C., Thompson, I. B., Sheckman, S. A. & Burley, G. S., 2006, *AJ*, 132, 85
- Prochaska, J. X., Naumos, S. O., Carney, B. W., McWilliam, A. & Wolfe, A. M., 2001, *AJ*, 120, 2513
- Ralchenko, Y., Jou, F.-C., Kelleher, D. E., Kramida, A. E., Musgrove, A., Reader, J., Wiese, W. L. & Olsen, K., 2007, *NIST Atomic Spectra Database*, online, <http://physics.nist.gov/asd3>
- Ramírez, S. V., Stephens, A., Frogel, J. A. & DePoy, D. L., 2000, *AJ*, 120, 833

- Reddy, B. E., Tomkink, J., Lambert D. L. & Allende Prieto, C., 2003, MNRAS, 340, 304
- Rich, R. M., 1988, AJ, 95, 828
- Rich, R. M. & Origlia, L., 2005, ApJ, 634, 1293
- Rich, R. M., Origlia, L. & Valenti, E., 2007, ApJ
- Sadler, E. M., Rich, R. M. & Terndrup, D. M., 1996, AJ, 112, 171
- Snedden, C., 1973, Ph.D. thesis, Univ. of Texas
- Snow, T. P. & Cohen, J. G., 1975, ApJ, 194, 313
- Takeda, Y., Zhao, G., Chen, YY. Q., Qiu, H. M. & Takada-Hidai, M., 2002, PASJ, 54, 275
- Trager, S. C., Faber, S. M., Worthey, G. & Jesus Gonzalez, J., 2000, AJ, 120, 165
- Tsujimoto, T., 2007, ApJ, in press (Astro-ph/0707.1168)
- Udalski, A. 2003, Acta Astron., 53, 291
- Udalski, A., et al. 2005, ApJ, 628, L109
- Vogt, S. E. et al. 1994, SPIE, 2198, 362
- Wallace, L., Hinkle, K. & Livingston, W. C., 1998, “An Atlas of the Spectrum of the Solar Photosphere from 13,500 to 28,000 cm^{-1} ”, N.S.O. Technical Report 98-001, <ftp://nsokp.nso.edu/pub/atlas/visatl>.
- Worthey, G., Faber, S. M., Gonzalez, J. J. & Burstein, D., 1994, ApJS, 94, 687
- Yi, S., Demarque, P., Kim, Y.-C. , Lee, Y.-W., Ree, C. Lejeune, Th. & Barnes, S., 2001, ApJS, 136, 417
- Zeigler, B.L., Thomas, D., Bohem, A., Bender, R., Fritz, A. & Maraston, C., 2005, A&A, 433, 519
- Zocalli, M. et al., 2003, A&A, 399, 931
- Zocalli, M. et al., 2004, A&A, 423, 507
- Zocalli, M. et al., 2006, A&A, 457, L1
- Zocalli, M., Hill, V., Lecureru, A., Barbuy, B., Renzini, A., Minitti, D., Gomez, A. & Ortolani, S., 2008, A&A, submitted

Table 1. W_λ for OGLE–2007–BLG–349S

λ (Å)	Species	EP (eV)	$\log(gf)$ (dex)	W_λ (mÅ)
6707.76	Li I	0.00	0.178	≤ 5.0
7111.45	C I	8.64	−1.000	21.2
7115.32	C I	8.64	−0.600	27.0
7116.96	C I	8.64	−1.000	21.8
6300.30	[O I]	0.00	−9.720	≤ 8.6
7771.94	O I	9.15	0.369	52.2
7774.17	O I	9.15	0.223	54.6
7775.39	O I	9.15	0.001	40.8
5682.63	Na I	2.10	−0.700	194.1
5688.19	Na I	2.10	−0.420	214.1
6154.23	Na I	2.10	−1.530	105.3
6160.75	Na I	2.00	−1.230	125.8
5711.09	Mg I	4.34	−1.670	168.8
6318.72	Mg I	5.11	−2.100	83.9
6319.24	Mg I	5.11	−2.320	66.2
6965.41	Mg I	5.75	−2.000 ^a	72.3
6696.02	Al I	3.14	−1.340	90.0
6698.67	Al I	3.14	−1.640	66.0
5701.10	Si I	4.93	−2.050	64.3
6145.02	Si I	5.61	−1.440	63.9
6155.13	Si I	5.62	−0.760	126.9
7235.33	Si I	5.61	−1.310 ^a	61.2
7235.82	Si I	5.61	−1.590 ^a	48.0
7800.00	Si I	6.18	−0.680 ^a	101.2
6756.96	S I	7.87	−0.90	syn
6757.15	S I	7.87	−0.31	syn
7698.97	K I	0.00	−0.168	240.0
5590.11	Ca I	2.52	−0.710	123.0
5867.56	Ca I	2.93	−1.340 ^a	60.0
6156.02	Ca I	2.52	−2.190	30.8
6161.30	Ca I	2.52	−1.030	104.5
6166.44	Ca I	2.52	−1.050	107.6

Table 1—Continued

λ (Å)	Species	EP (eV)	$\log(gf)$ (dex)	W_λ (mÅ)
6169.04	Ca I	2.52	−0.540	144.7
6455.60	Ca I	2.52	−1.360	97.1
6464.68	Ca I	2.52	−2.150 ^a	47.7
6471.66	Ca I	2.52	−0.590	124.8
6499.65	Ca I	2.54	−0.590	130.3
6798.48	Ca I	2.71	−2.420 ^a	31.5
5684.20	Sc II	1.51	−1.080	54.5
6245.64	Sc II	1.51	−1.130	49.5
5453.64	Ti I	1.44	−1.610	27.0
5648.57	Ti I	2.49	−0.252	44.5
5739.46	Ti I	2.25	−0.602	35.1
5766.33	Ti I	3.29	0.360	35.8
5913.73	Ti I	0.02	−3.780 ^a	8.0
5918.54	Ti I	1.07	−1.470	52.7
6092.80	Ti I	1.89	−1.380	21.5
6716.67	Ti I	2.49	−1.060 ^a	9.7
6606.95	Ti II	2.06	−2.790	18.6
5670.85	V I	1.08	−0.425	68.6
6081.44	V I	1.05	−0.579	67.6
6090.22	V I	1.08	−0.062	90.4
6251.82	V I	0.29	−1.340	81.7
6285.14	V I	0.28	−1.510	52.4
5702.32	Cr I	3.45	−0.667	66.0
5783.09	Cr I	3.32	−0.500	61.0
5783.89	Cr I	3.32	−0.295	84.9
5787.96	Cr I	3.32	−0.083	73.2
5844.59	Cr I	3.01	−1.760	21.0
6978.49	Cr I	3.46	0.143	127.0
6979.80	Cr I	3.46	−0.411	73.4
5537.74	Mn I	2.19	−2.020	133.3
6013.50	Mn I	3.07	−0.252	145.9
6021.80	Mn I	3.08	0.034	163.3

Table 1—Continued

λ (Å)	Species	EP (eV)	$\log(gf)$ (dex)	W_λ (mÅ)
5916.25	Fe I	2.45	−2.910	91.2
5927.79	Fe I	4.65	−0.990	66.2
5929.67	Fe I	4.55	−1.310	70.5
5930.17	Fe I	4.65	−0.140	131.6
5934.65	Fe I	3.93	−1.070	112.2
5940.99	Fe I	4.18	−2.050	42.8
5952.72	Fe I	3.98	−1.340	100.8
5956.69	Fe I	0.86	−4.500	88.8
5976.79	Fe I	3.94	−1.330	98.0
5983.69	Fe I	4.55	−0.660	101.6
5984.83	Fe I	4.73	−0.260	130.4
6024.05	Fe I	4.55	0.030	161.0
6027.05	Fe I	4.07	−1.090	89.2
6055.99	Fe I	4.73	−0.370	99.5
6065.48	Fe I	2.61	−1.410	179.7
6078.50	Fe I	4.79	−0.330	112.2
6079.00	Fe I	4.65	−1.020	73.1
6089.57	Fe I	5.02	−0.900	61.8
6093.67	Fe I	4.61	−1.400	54.7
6094.37	Fe I	4.65	−1.840	48.0
6096.66	Fe I	3.98	−1.830	70.1
6120.25	Fe I	0.92	−5.970	24.3
6127.90	Fe I	4.14	−1.400	76.1
6136.99	Fe I	2.20	−2.950	109.5
6151.62	Fe I	2.18	−3.370	80.3
6157.73	Fe I	4.07	−1.160	92.4
6159.37	Fe I	4.61	−1.920	34.9
6165.36	Fe I	4.14	−1.470	71.8
6173.34	Fe I	2.22	−2.880	107.1
6180.20	Fe I	2.73	−2.650	92.4
6187.99	Fe I	3.94	−1.620	87.2
6200.31	Fe I	2.61	−2.370	97.5

Table 1—Continued

λ (Å)	Species	EP (eV)	$\log(gf)$ (dex)	W_λ (mÅ)
6232.64	Fe I	3.65	−1.220	128.9
6240.65	Fe I	2.22	−3.170	81.9
6246.32	Fe I	3.60	−0.880	177.9
6252.55	Fe I	2.40	−1.770	174.2
6265.13	Fe I	2.18	−2.540	130.6
6271.28	Fe I	3.33	−2.700	52.0
6290.97	Fe I	4.73	−0.730	108.6
6297.79	Fe I	2.22	−2.640	116.0
6301.51	Fe I	3.65	−0.718	181.6
6302.50	Fe I	3.69	−1.110	126.0
6311.50	Fe I	2.83	−3.140	71.6
6315.31	Fe I	4.14	−1.230	111.4
6315.81	Fe I	4.07	−1.610	71.4
6322.69	Fe I	2.59	−2.430	121.3
6336.82	Fe I	3.69	−0.856	167.1
6355.03	Fe I	2.84	−2.290	108.5
6380.75	Fe I	4.19	−1.380	85.7
6392.54	Fe I	2.28	−3.990	49.6
6408.03	Fe I	3.69	−1.020	155.0
6430.84	Fe I	2.18	−1.950	175.5
6436.41	Fe I	4.19	−2.450	34.6
6475.63	Fe I	2.56	−2.940	97.9
6481.87	Fe I	2.28	−3.010	105.7
6483.94	Fe I	1.48	−5.340	18.7
6495.74	Fe I	4.83	−0.840	66.5
6498.94	Fe I	0.96	−4.690	90.5
6518.37	Fe I	2.83	−2.450	88.9
6533.93	Fe I	4.56	−1.360	71.3
6546.24	Fe I	2.76	−1.540	154.3
6581.21	Fe I	1.48	−4.680	63.2
6592.91	Fe I	2.73	−1.470	165.9
6593.87	Fe I	2.43	−2.370	124.8

Table 1—Continued

λ (Å)	Species	EP (eV)	$\log(gf)$ (dex)	W_λ (mÅ)
6597.56	Fe I	4.79	−0.970	72.6
6608.02	Fe I	2.28	−3.930	49.2
6609.11	Fe I	2.56	−2.660	109.2
6625.02	Fe I	1.01	−5.370	54.8
6627.54	Fe I	4.55	−1.580	61.8
6633.75	Fe I	4.79	−0.800	102.0
6646.93	Fe I	2.61	−3.960	38.5
6653.91	Fe I	4.15	−2.520	24.3
6699.15	Fe I	4.59	−2.100	24.1
6703.57	Fe I	2.76	−3.060	73.2
6710.32	Fe I	1.48	−4.870	53.2
6713.77	Fe I	4.79	−1.500	45.0
6715.38	Fe I	4.61	−1.540	73.1
6716.22	Fe I	4.58	−1.850	51.5
6725.35	Fe I	4.19	−2.250	39.9
6726.67	Fe I	4.61	−1.070	78.0
6733.15	Fe I	4.64	−1.480	53.4
6739.52	Fe I	1.56	−4.790	42.2
6745.11	Fe I	4.58	−2.170	27.8
6746.95	Fe I	2.61	−4.300	15.4
6750.15	Fe I	2.42	−2.580	116.5
6752.71	Fe I	4.64	−1.200	78.2
6806.86	Fe I	2.73	−3.210	75.1
6837.02	Fe I	4.59	−1.690	39.4
6839.83	Fe I	2.56	−3.350	67.2
6842.68	Fe I	4.64	−1.220	68.8
6843.65	Fe I	4.55	−0.830	94.3
6851.63	Fe I	1.61	−5.280	21.3
6855.18	Fe I	4.56	−0.740	105.8
6855.71	Fe I	4.61	−1.780	43.5
6858.15	Fe I	4.61	−0.930	77.4
6861.95	Fe I	2.42	−3.850	60.2

Table 1—Continued

λ (Å)	Species	EP (eV)	$\log(gf)$ (dex)	W_λ (mÅ)
6862.49	Fe I	4.56	−1.470	60.1
6971.93	Fe I	3.02	−3.340	41.2
6978.85	Fe I	2.48	−2.450	114.6
6988.52	Fe I	2.40	−3.560	71.3
6999.88	Fe I	4.10	−1.460	94.5
7000.62	Fe I	4.14	−2.390	50.2
7007.96	Fe I	4.18	−1.960	64.8
7014.98	Fe I	2.45	−4.200	31.0
7022.95	Fe I	4.19	−1.150	98.7
7038.22	Fe I	4.22	−1.200	109.0
7112.17	Fe I	2.99	−3.000	79.6
7114.55	Fe I	2.69	−4.000	27.7
7130.92	Fe I	4.22	−0.750	147.5
7132.98	Fe I	4.07	−1.630	71.4
7142.52	Fe I	4.95	−1.030	80.7
7179.99	Fe I	1.48	−4.750	60.7
7189.15	Fe I	3.07	−2.770	82.0
7285.27	Fe I	4.61	−1.660	54.7
7306.56	Fe I	4.18	−1.690	79.9
7401.69	Fe I	4.19	−1.350	70.2
7418.67	Fe I	4.14	−1.380	84.5
7440.92	Fe I	4.91	−0.720	92.9
7443.02	Fe I	4.19	−1.780	73.2
7447.40	Fe I	4.95	−1.090	65.3
7454.00	Fe I	4.19	−2.370	41.2
7461.52	Fe I	2.56	−3.530	66.1
7563.02	Fe I	4.83	−1.660	44.0
7568.91	Fe I	4.28	−0.940	121.7
7583.79	Fe I	3.02	−1.890	128.0
7586.04	Fe I	4.31	−0.130	185.1
7710.36	Fe I	4.22	−1.110	108.0
7723.30	Fe I	2.28	−3.610	86.9

Table 1—Continued

λ (Å)	Species	EP (eV)	$\log(gf)$ (dex)	W_λ (mÅ)
7748.27	Fe I	2.95	−1.750	166.7
7751.12	Fe I	4.99	−0.850	84.3
7780.57	Fe I	4.47	−0.040	186.1
7807.92	Fe I	4.99	−0.620	99.2
7941.08	Fe I	3.27	−2.290	69.7
8239.13	Fe I	2.42	−3.180	83.5
8293.49	Fe I	3.30	−2.180	91.2
5197.58	Fe II	3.23	−2.230	78.6
5234.63	Fe II	3.22	−2.220	85.1
5991.38	Fe II	3.15	−3.570	38.3
6084.11	Fe II	3.20	−3.800	25.5
6149.26	Fe II	3.89	−2.690	38.9
6247.56	Fe II	3.89	−2.360	48.3
6369.46	Fe II	2.89	−4.200	22.4
6416.92	Fe II	3.89	−2.690	46.2
6432.68	Fe II	2.89	−3.740	36.5
6456.39	Fe II	3.90	−2.310	55.6
6516.08	Fe II	2.89	−3.450	54.2
5530.79	Co I	1.71	−2.060	74.0
5647.23	Co I	2.28	−1.560	51.5
6189.00	Co I	1.71	−2.450	47.1
6632.45	Co I	2.28	−2.000	42.2
7417.41	Co I	2.04	−2.070	49.4
6053.69	Ni I	4.23	−1.070	41.9
6086.28	Ni I	4.26	−0.515	79.1
6128.97	Ni I	1.68	−3.330	61.8
6130.13	Ni I	4.26	−0.959	48.4
6175.37	Ni I	4.09	−0.535	77.5
6176.81	Ni I	4.09	−0.529	96.5
6177.24	Ni I	1.83	−3.510	41.7
6186.71	Ni I	4.10	−0.965	57.0
6204.60	Ni I	4.09	−1.140	58.9

Table 1—Continued

λ (Å)	Species	EP (eV)	$\log(gf)$ (dex)	W_λ (mÅ)
6360.82	Ni I	4.17	−1.150	39.6
6370.35	Ni I	3.54	−1.940	41.1
6378.25	Ni I	4.15	−0.899	60.6
6482.80	Ni I	1.93	−2.630	86.9
6586.31	Ni I	1.95	−2.810	85.7
6598.60	Ni I	4.23	−0.978	54.4
6635.12	Ni I	4.42	−0.828	53.6
6643.63	Ni I	1.68	−2.300	143.2
6767.77	Ni I	1.83	−2.170	121.1
6772.31	Ni I	3.66	−0.987	85.0
6842.04	Ni I	3.66	−1.470	50.1
7422.27	Ni I	3.63	−0.129	153.6
7797.59	Ni I	3.90	−0.180	121.7
5782.12	Cu I	1.64	−1.780	142.6
6362.34	Zn I	5.79	0.140	29.3
7800.29	Rb I	0.00	0.13	syn
6127.44	Zr I	0.15	−1.06	18.0
6134.55	Zr I	0.00	−1.28	16.2
6143.20	Zr I	0.07	−1.10	20.4
5853.70	Ba II	0.60	−1.01	66.3
6141.70	Ba II	0.70	−0.07	130.0
6496.90	Ba II	0.60	−0.38	108.4
6390.48	La II	0.32	−1.41	12.6
6774.26	La II	0.13	−1.72	10.8
6645.11	Eu II	1.38	0.12	15.4

^aAn inverted solar analysis was used to determine gf .

Table 2. Abundances in OGLE-2007-BLG-349S

Species	$\log[\epsilon(X)]^a$ (dex)	σ_{obs}^b (dex)	Num. of Lines	$\log[\epsilon(X)/\epsilon(X)_\odot]$ (dex)	$[X/Fe]^k$ colhead(dex)	σ_{pred} for $[X/Fe]$ (dex)	Notes
Li I	≤ 0.86	...	1	$\leq +0.06$	≤ -0.45	0.13	syn
C I	8.92	0.07	3	+0.31	-0.12	0.21	high χ
C(CH)	9.05	0.15	band	+0.39	-0.12	0.17	syn
O I	9.07	0.12	3	+0.14	-0.29	0.19	high χ
Na I	6.64	0.11	4	+0.77	+0.26	0.09	
Mg I	8.16	0.10	4	+0.59	+0.08	0.07	
Al I	6.82	0.04	2	+0.49	+0.13	0.08	
Si I	8.00	0.12	6	+0.47	+0.04	0.17	high χ
S I	7.62	...	1 ^h	+0.45	+0.02	0.20	syn, high χ
K I	5.61	...	1	+0.38	-0.13	0.12	c
Ca I	6.58	0.14	11	+0.55	+0.04	0.07	
Sc II	3.71	0.03	2	+0.54	+0.13	0.10	d
Ti I	5.36	0.12	8	+0.53	+0.02	0.11	
Ti II	5.57	...	1	+0.67	+0.24	0.10	
V I	4.47	0.06	5	+0.68	+0.17	0.14	d
Cr I	6.19	0.11	7	+0.53	+0.02	0.07	
Mn I	6.03	0.11	3	+0.66	+0.15	0.11	e
Fe I	7.97	0.15	135	+0.51	0.00	0.09 ⁱ	
Fe II	7.92	0.10	11	+0.43	-0.08	0.17 ^j	
Co I	5.55	0.14	5	+0.77	+0.26	0.08	d
Ni I	6.86	0.13	22	+0.67	+0.16	0.05	
Cu I	4.74	...	1	+0.79	+0.28	0.15	f
Zn I	4.97	...	1	+0.42	-0.09	0.13	
Rb I	3.40	0.15	1	+0.77	+0.26	0.17	syn
Zr I	3.28	0.01	3	+0.39	-0.14	0.16	
Ba II	2.50	0.05	3	+0.38	-0.05	0.17	d
La II	1.98	0.01	2	+0.97	+0.54	0.12	g
Eu II	1.38	...	1	+0.88	+0.45	0.10	g

^aThis is $\log[(n(X)/n(H)) + 12.0]$ dex.

^bRms dispersion about the mean abundance, using differential line-by-line abundances with respect to the

Sun.

^cA 0.08 dex non-LTE correction relative to the Sun is included for K I.

^dThe HFS corrections are small and not an issue.

^eThe HFS corrections are large and are a concern.

^fThe HFS corrections are very large and are a major concern.

^gOnly one or two very weak lines detected. Could be upper limits.

^hVery close pair of lines on wing of much stronger Si I line.

ⁱThe uncertainty in $[\text{Fe}/\text{H}]$ inferred from the 135 Fe I lines.

^jThe uncertainty in $[\text{Fe}/\text{H}]$ inferred from the 11 Fe II lines.

^kThe reference species (Fe I or Fe II) is given in Table 4.

Table 3. Sensitivity of Deduced Absolute Abundances

Species	$\Delta \log[\epsilon(x)]$ for $\Delta T_{\text{eff}} + 250 \text{ K}$ (dex)	$\Delta \log[\epsilon(x)]$ for $\Delta \log(g) + 0.5 \text{ dex}$ (dex)	$\Delta \log[\epsilon(x)]$ for $\Delta v_t = +0.2 \text{ km s}^{-1}$ (dex)	$\Delta \log[\epsilon(x)]$ for $\Delta [\text{Fe}/\text{H}] \text{ model} + 0.5 \text{ dex}$ (dex)
Li I	0.27	−0.02	0.00	0.01
O I ^a	−0.01	0.25	0.00	0.22
O I ^b	−0.32	0.17	−0.01	0.03
C I	−0.29	0.17	−0.01	0.00
CH	0.20	−0.11	−0.05	0.04
Na I	0.18	−0.19	−0.02	0.12
Mg I	0.08	−0.09	−0.03	0.06
Al I	0.14	−0.06	−0.03	0.04
Si I	−0.07	−0.01	−0.02	0.10
S I	−0.21	0.16	−0.01	0.01
K I	0.25	−0.24	−0.03	0.15
Ca I	0.20	−0.11	−0.05	0.07
Sc II	−0.02	0.22	−0.04	0.18
Ti I	0.25	−0.01	−0.02	0.02
Ti II	−0.05	0.22	−0.02	0.17
V I	0.33	−0.03	−0.07	−0.01
Cr I	0.18	−0.08	−0.04	0.06
Mn I	0.20	−0.18	−0.07	0.16
Fe I	0.12	−0.04	−0.05	0.10
Fe II	−0.19	0.24	−0.05	0.19
Ni I	0.06	0.00	−0.05	0.13
Co I	0.12	0.05	−0.05	0.07
Cu I	0.17	−0.11	−0.07	0.24
Zn I	−0.13	0.13	−0.03	0.12
Rb I	0.22	−0.03	−0.03	0.00
Zr I	0.35	−0.02	−0.01	0.00
Ba II	0.06	0.09	−0.11	0.26
La II	0.04	0.22	−0.01	0.20
Eu II	−0.02	0.22	−0.02	0.18

^afor 6300 Å line of [OI], only an upper limit here.

^bfor the three lines of the 7770 Å O I triplet.

Table 4. Sensitivity of Deduced Relative Abundances

Species	$\Delta[X/\text{Fe}]$ for $\Delta T_{\text{eff}} + 250 \text{ K}$ (dex)	$\Delta[X/\text{Fe}]$ for $\Delta \log(g) + 0.5 \text{ dex}$ (dex)	$\Delta[X/\text{Fe}]$ for $\Delta v_t = +0.2 \text{ km s}^{-1}$ (dex)	$\Delta[X/\text{Fe}]$ for $\Delta [\text{Fe}/\text{H}] \text{ model} + 0.5 \text{ dex}$ (dex)	Ref. ^a
Li I	0.15	0.02	0.05	−0.09	1
O I ^b	−0.13	0.29	0.05	0.12	1
O I ^c	−0.13	−0.07	0.04	−0.16	2
C I	−0.10	−0.07	0.04	−0.19	2
CH	0.08	−0.07	0.00	−0.06	1
Na I	0.06	−0.15	0.03	0.02	1
Mg I	−0.04	−0.05	0.02	−0.04	1
Al I	0.02	−0.02	0.02	−0.06	1
Si I	0.12	−0.25	0.03	−0.09	2
S I	−0.02	−0.08	0.04	−0.18	2
K I	0.13	−0.20	0.02	0.05	1
Ca I	0.08	−0.07	0.00	−0.03	1
Sc II	0.17	−0.02	0.01	−0.01	2
Ti I	0.13	0.03	0.03	−0.08	1
Ti II	0.14	−0.02	0.03	−0.02	2
V I	0.21	0.01	−0.02	−0.11	1
Cr I	0.06	−0.04	0.01	−0.04	1
Mn I	0.08	−0.14	−0.02	0.06	1
Co I	0.00	0.09	0.00	−0.03	1
Ni I	−0.06	0.04	0.00	0.03	1
Cu I	0.05	−0.07	−0.02	0.14	1
Zn I	−0.25	0.17	0.02	0.02	1
Rb I	0.10	0.01	0.02	−0.10	1
Ba II	0.25	−0.15	−0.06	0.07	2
Zr I	0.23	0.02	0.04	−0.10	1
La II	0.23	−0.02	0.04	0.01	2
Eu II	0.17	−0.02	0.03	−0.01	2

^a1 denotes a value of $[X/\text{Fe}]$ where Fe I is used as the reference, while for 2, Fe II is used.

^bfor 6300 Å line of [OI], only an upper limit here.

^cfor the three lines of the 7770 Å O I triplet.

Table 5. Diffuse Interstellar Bands in OGLE–2007–BLG–349S

Wavelength (Å)	FWHM (Å)	W_λ (mÅ)	Central Depth (%)
5778 ^a	9	1300	0.14
5778 ^b	1.8	330	0.19
6008	3.9	400	0.08
6282	4.3	2000	0.30
6611	1.5	200	0.14

^awide component of blend

^bnarrow component of blend

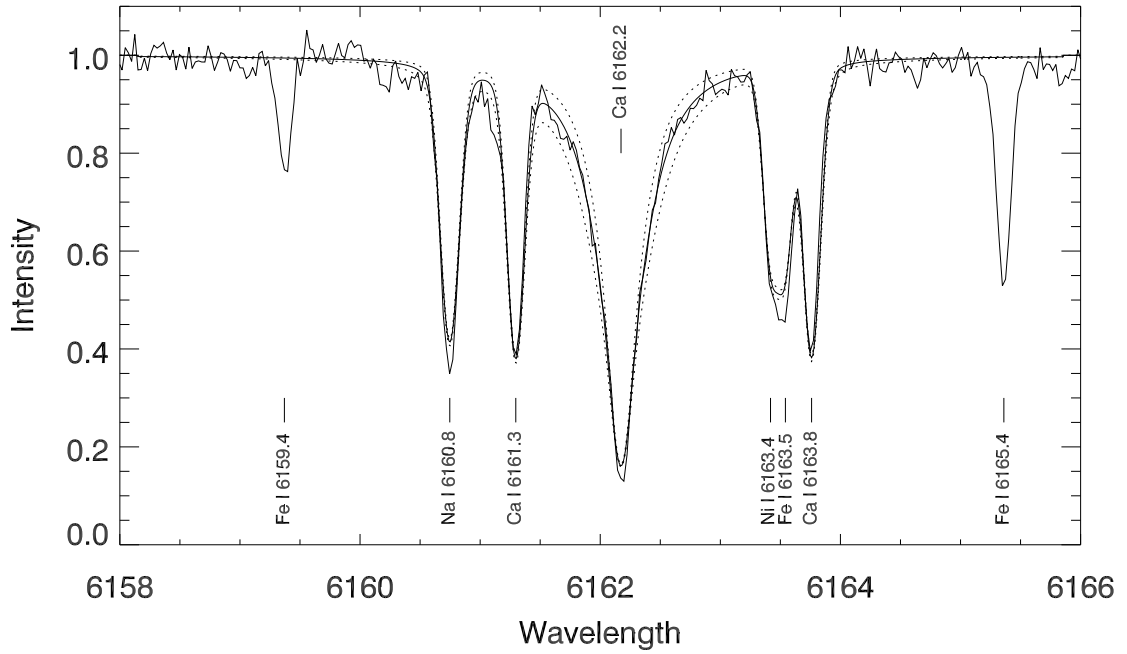


Fig. 1.— The spectrum of OGLE-2007-BLG-349S in the region of the strong Ca I line at 6162.2 Å is shown shifted to the rest frame. Overplotted as a thick line is a spectral synthesis covering 5160 to 5165 Å for $T_{\text{eff}} = 5400$ K, $[\text{Fe}/\text{H}] = +0.5$ dex, and solar $[\text{Ca}/\text{Fe}]$ with the best fit $\log(g)$ of 4.35 dex. The thin dashed lines represent offsets in $\log(g)$ of ± 0.3 dex.

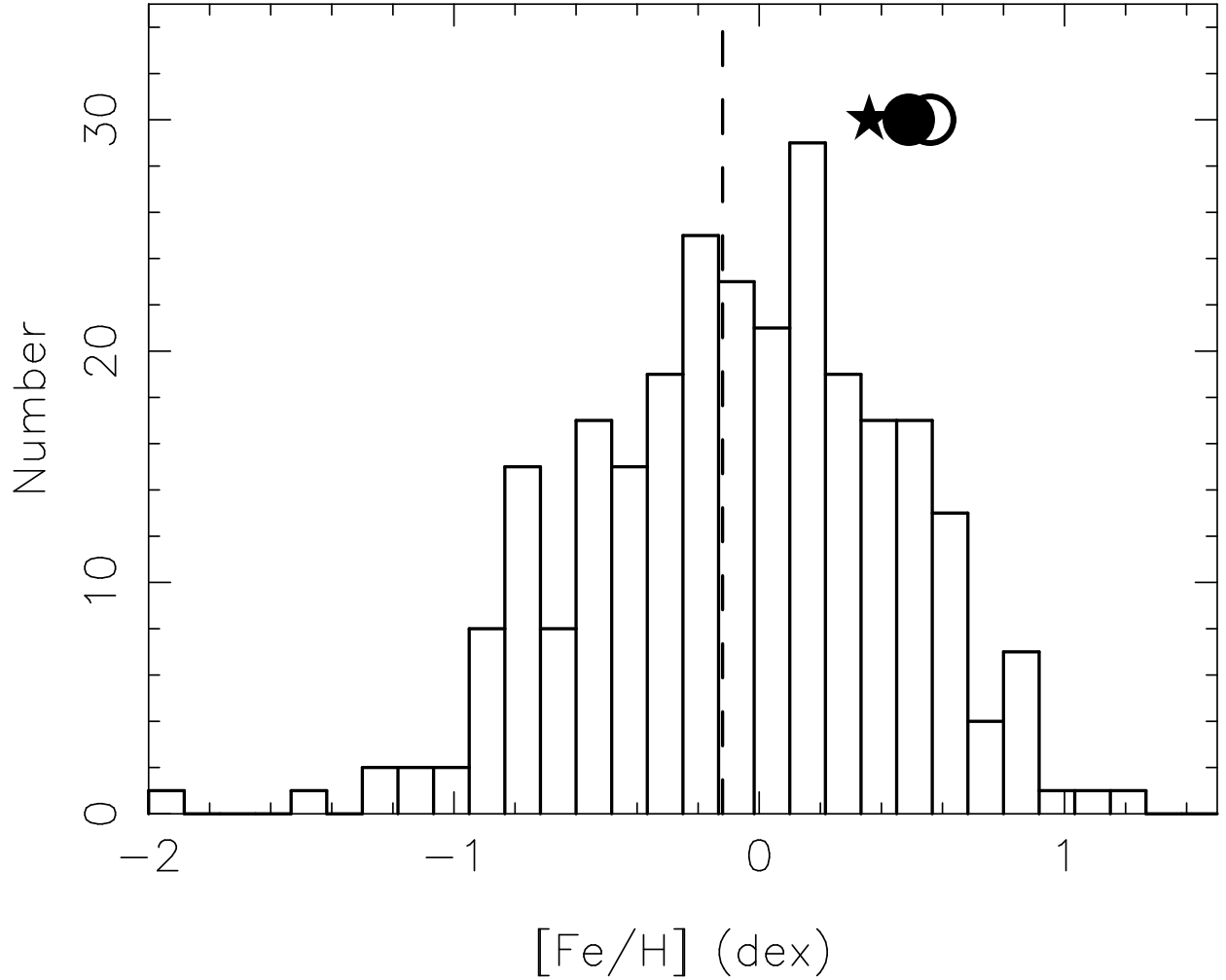


Fig. 2.— Fe-metallicity distribution for the sample of 268 Galactic bulge stars from Sadler, Rich & Terndrup (1996) as re-calibrated by Fulbright, McWilliam & Rich (2006) is shown. The median at $[\text{Fe}/\text{H}] -0.12$ dex is indicated by the dashed vertical line. The $[\text{Fe}/\text{H}]$ values for the three microlensed bulge dwarfs, OGLE-2007-BLG-349S studied here (large filled circle), OGLE-2006-BLG-265S (Johnson et al. 2007) (large open circle), and MOA-2006-BLG-099S (Johnson et al. 2008) (star symbol), are marked.

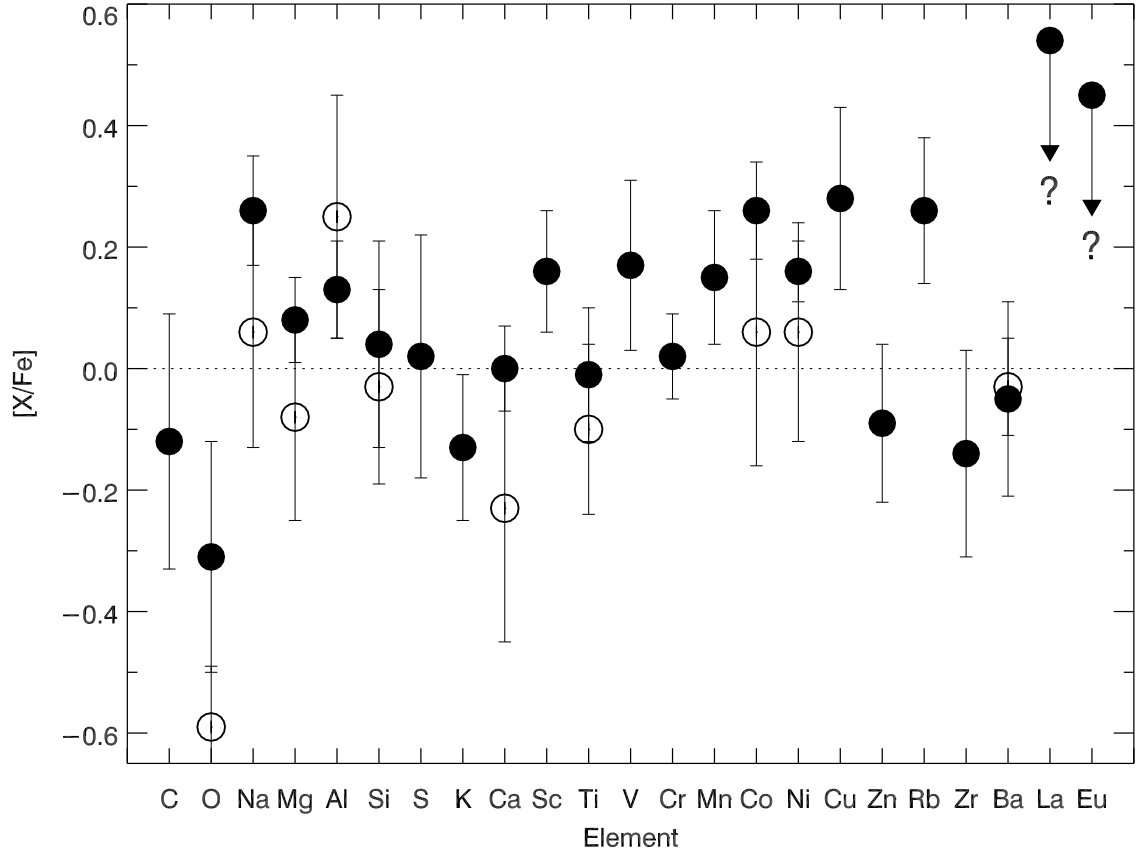


Fig. 3.— Abundance ratios for various species are shown for OGLE-2007-BLG-349S analyzed here (filled circles) and for OGLE-2006-BLG-265S (open circles) from Johnson et al. (2007).

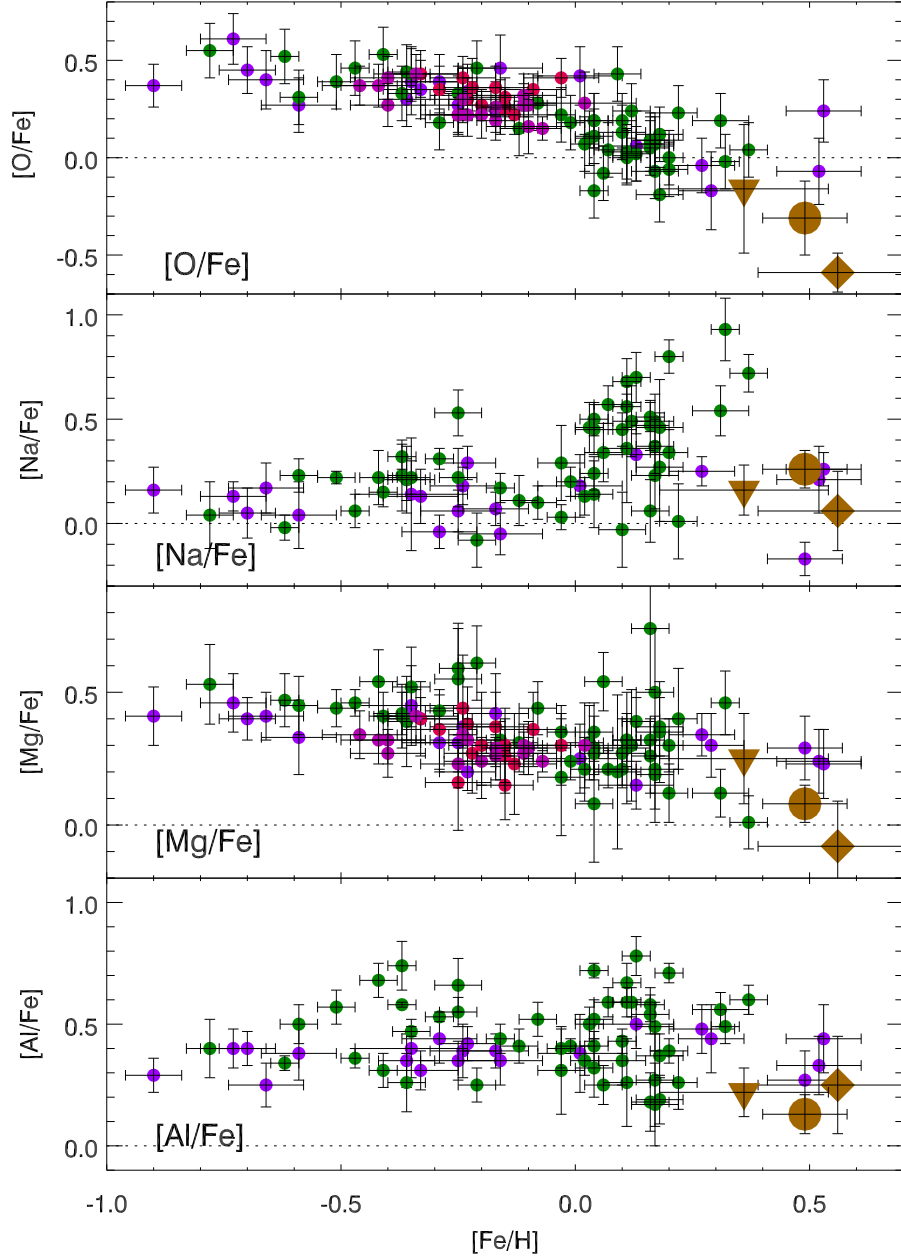


Fig. 4.— Abundance ratios $[\text{O}/\text{Fe}]$, $[\text{Na}/\text{Fe}]$, $[\text{Mg}/\text{Fe}]$ and $[\text{Al}/\text{Fe}]$ are shown as a function of $[\text{Fe}/\text{H}]$. The three microlensed stars are indicated by large brown symbols: OGLE-2007-BLG-349S (filled circle), OGLE-2006-BLG-265S from Johnson et al. (2007) (diamond), and MOA-2006-BLG-099S from Johnson et al. (2008) (inverted triangle). They are shown superposed on those for samples of bulge M and K giants of Fulbright, McWilliam & Rich (2007) (blue circles), Rich & Origlia (2005) (red circles), Lecureur et al. (2007) (green circles), and for M giants in the inner bulge from Rich, Origlia & Valenti (2007) (pink circles).

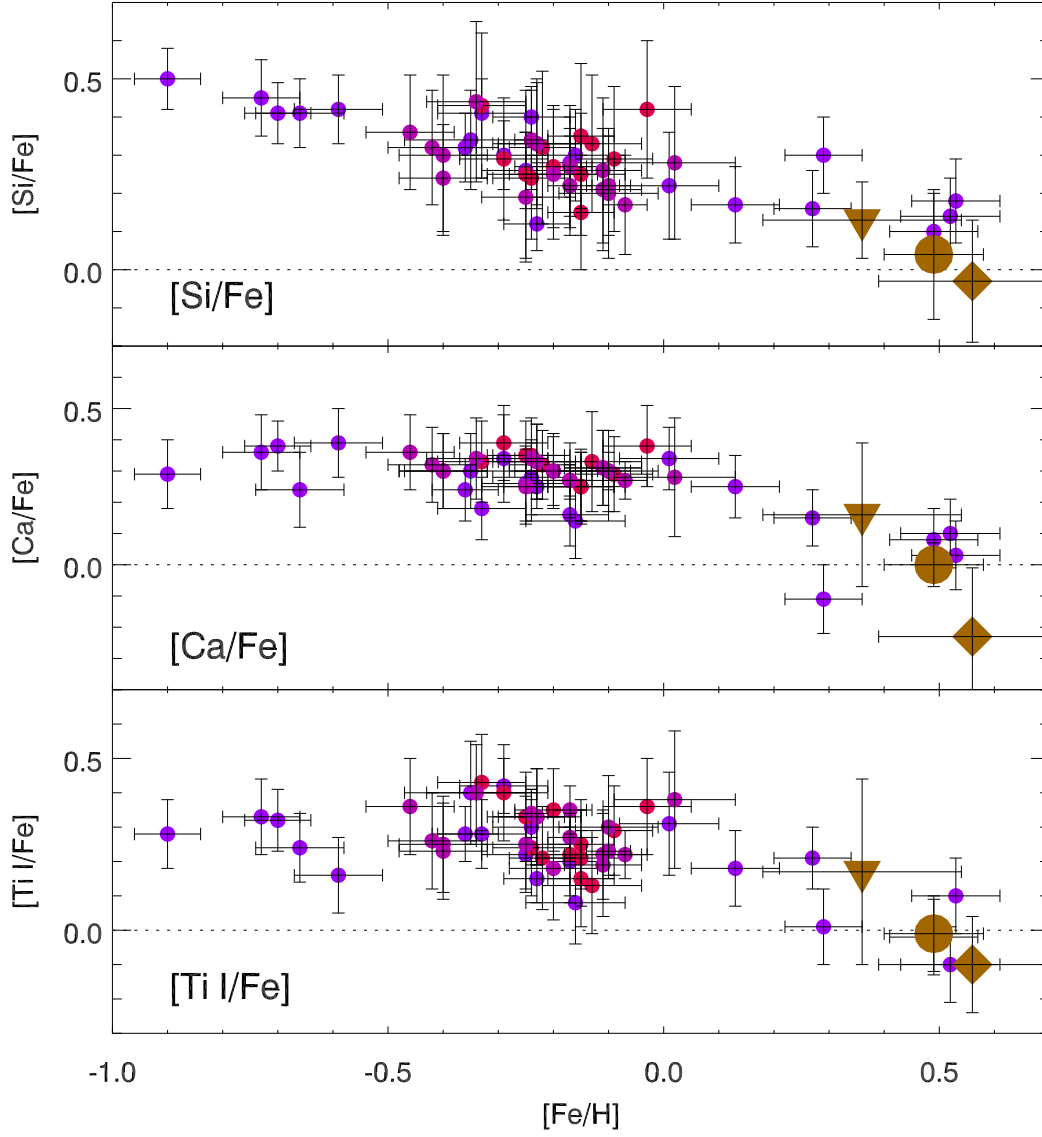


Fig. 5.— The same as Fig. 4 for $[\text{Si}/\text{Fe}]$, $[\text{Ca}/\text{Fe}]$ and $[\text{Ti I}/\text{Fe}]$. The symbols are the same as in Fig. 4.

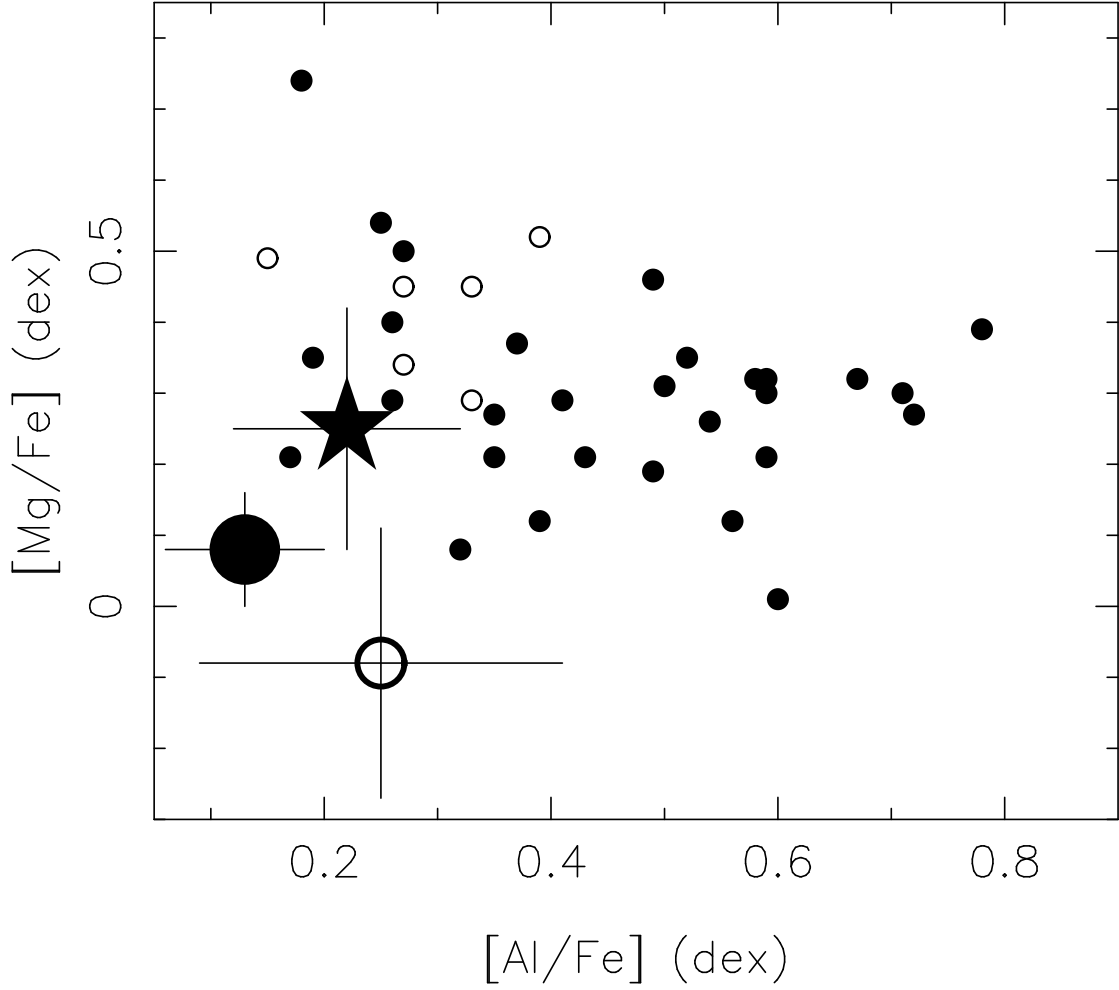


Fig. 6.— The $[\text{Mg}/\text{Fe}]$ ratio versus the $[\text{Al}/\text{Fe}]$ ratio for OGLE–2007–BLG–349S, analyzed here, is shown as the large filled circle, OGLE–2006–BLG–265S from Johnson et al. (2007) as the large open circle, and MOA–2006–BLG–099S from Johnson et al. (2008) as the large star. Those stars with $[\text{Fe}/\text{H}] > 0.0$ dex from the samples of bulge giants and red clump stars of Lecureur et al. (2007) are shown as small filled circles, and those from the sample of Fulbright, McWilliam & Rich (2007) as small open circles. Error bars (1σ) are shown for the three OGLE dwarfs; those of the two samples of bulge giants are similar to those for OGLE–2006–BLG–265S taken from Johnson et al. (2007).